Research Square

Preprints are preliminary reports that have not undergone peer review.
They should not be considered conclusive, used to inform clinical practice,
or referenced by the media as validated information.

Carbocation-Guided Regioselective Deoxygenation of Unsymmetrical Diols via B(C6F5)3 Catalysis with Silane Economy

Jeonghyo Lee

jeonghyolee@hanyang.ac.kr

Hanyang University https://orcid.org/0000-0002-7985-7503

Article

Keywords:

Posted Date: July 7th, 2026

DOI: https://doi.org/10.21203/rs.3.rs-8536759/v1

License: This work is licensed under a Creative Commons Attribution 4.0 International License.
Read Full License

Additional Declarations: There is **NO** Competing Interest.

Carbocation-Guided Regioselective Deoxygenation of Unsymmetrical Diols via $B(C_6F_5)_3$ Catalysis with Silane Economy

Sojeong Bang,[1] Jooye Lee,[1,2] Daseop Jo,[1,2] Yewon Kim,[1] and Jeonghyo Lee[1*]

[1]Department of Chemistry and Research Institute for Convergence of Basic Science, Hanyang University, Seoul 04763, Republic of Korea.

[2]These authors contributed equally to this work

*e-mail: jeonghyolee@hanyang.ac.kr

Abstract

Selective deoxygenation of polyhydroxylated compounds remains a persistent challenge, particularly at sterically hindered sites of unsymmetrical diols. Herein, we report a $B(C_6F_5)_3$/silane catalytic system that achieves deoxygenation at sterically demanding sites under mild conditions using substoichiometric hydrosilane. Mechanistic studies revealed that the reaction proceeds through an S_N1-type pathway involving carbocation formation at tertiary centers, accounting for the observed selectivity. Diphenylsilane was identified as the optimal silane, whose dual hydride-donor capacity enables effective operation under substoichiometric loading and ensures high silane economy. The utility of this system was further demonstrated through benzylic deuteration, providing a practical entry to isotopically labelled molecules. Collectively, these findings establish a versatile framework for site-selective alcohol deoxygenation and broaden opportunities in selective C–O bond cleavage within polyhydroxylated systems.

Introduction

Polyols, defined by the presence of multiple hydroxyl groups, are ubiquitous structural motifs found in natural products,[1] biomass-derived compounds,[2, 3] and synthetic intermediates.[4, 5] Their dense hydroxyl functionality, however, often complicates selective structural modification,[6-8] typically requiring laborious, step-intensive protecting-group manipulations.[9, 10] To streamline access to structurally diverse derivatives, chemists have focused on developing direct,[11, 12] site-selective transformations of polyhydroxylated compounds.[13-21] Among these, the selective deoxygenation of polyols has emerged as a particularly powerful strategy.[22-25] By directly converting hydroxyl groups into C–H bonds, this process provides a shortcut to simplified scaffolds while retaining stereochemical complexity, a feature highly valued in drug discovery, natural product synthesis, and materials innovation.[26]

In this context, Lewis acid/silane combinations represent a well-established class of systems for alcohol deoxygenation and have therefore been considered as potential platforms for selective C–O bond clevage.[27, 28] In such systems, selectivity is dictated by the mode of C–O bond activation, leading to distinct reactivity patterns depending on the Lewis acid employed. Conventional Lewis acids, such as In,[29-32] Pd,[33] Sc,[34] or Ti[35, 36]-based catalysts, typically engage the hydroxyl group directly, promoting heterolytic C–O bond scission through pathways involving carbocation formation. As a consequence, deoxygenation preferentially occurs at more substituted alcohols, consistent with the intrinsic carbocation stability trend (3° > 2° > 1°). (**Fig. 1A**) In sharp contrast, tris(pentafluorophenyl)borane, $B(C_6F_5)_3$, exhibits a fundamentally different reactivity profile. Rather than activating the alcohol substrate, this boron Lewis acid selectively engages the hydrosilane, and subsequent reduction proceeds via hydride transfer to an alcohol-derived intermediate.[37-40] Since hydride

delivery is most effective at sterically accessible sites, $B(C_6F_5)_3$-catalysed deoxygenation displays an inverted selectivity trend, favoring primary alcohols over secondary and tertiary ones.[41, 42]

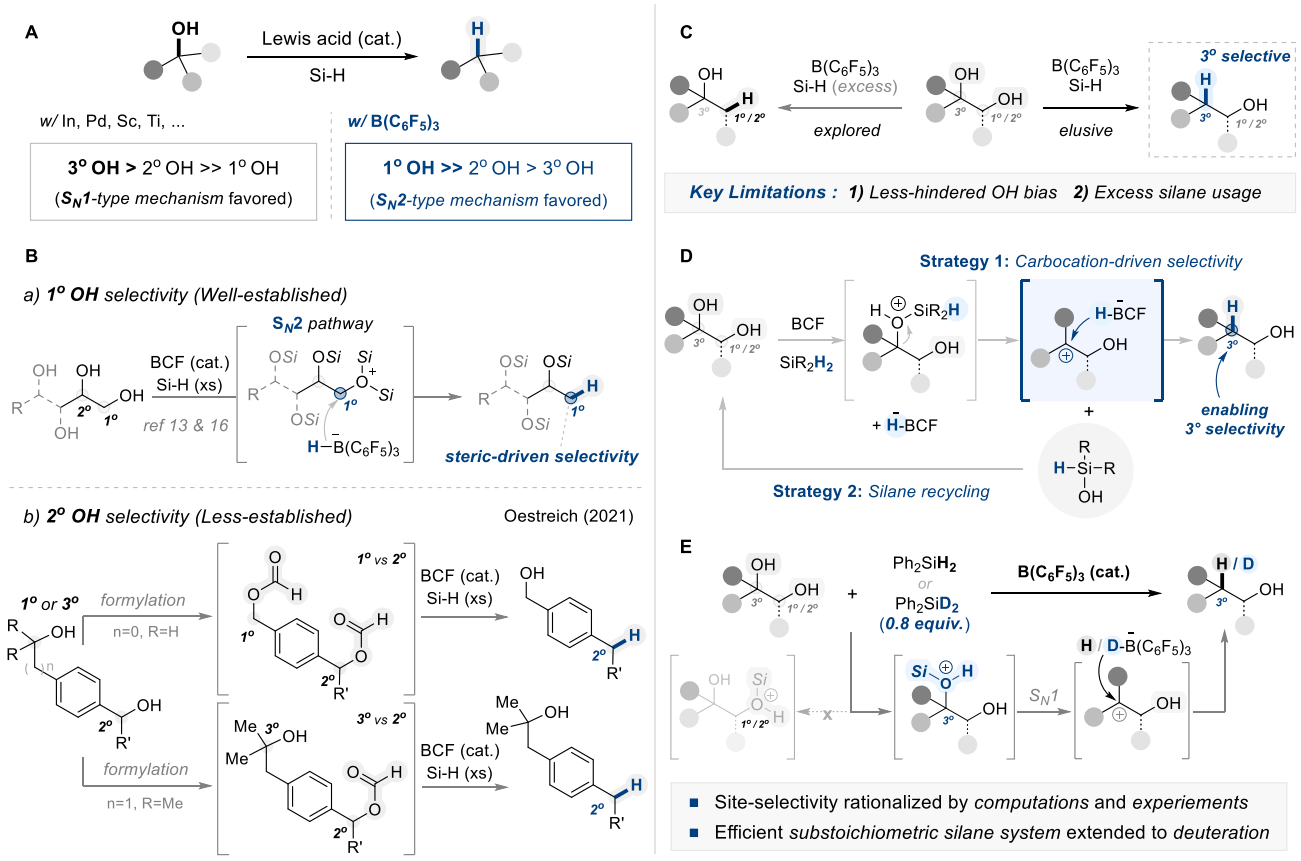


Fig. 1 | Reactivity trends and design strategy for site-selective deoxygenation of polyols under $B(C_6F_5)_3$–hydrosilane catalysis A. Selectivity in Lewis acid/hydrosilane-mediated alcohol deoxygenation **B.** Selectivity trends in BCF/hydrosilane-mediated polyol deoxygenation **C.** Limitations in BCF/hydrosilane-promoted polyol deoxygenation **D.** Our strategies to address challenges in BCF/hydrosilane deoxygenation **E.** This work: Site-selective deoxygenation of unsymmetrical diols

When applied to polyhydroxylated substrates, this inherent selectivity becomes particularly pronounced. Competition among multiple hydroxyl groups under identical reaction conditions directs deoxygenation almost exclusively to the least hindered primary position, rendering $B(C_6F_5)_3$/silane combinations a general and reliable approach for primary-selective deoxygenation of polyols (**Fig. 1B**-a).[43-49] Beyond this dominant trend, the Oestreich group demonstrated that secondary alcohol deoxygenation can be achieved in selected cases by employing a prefunctionalization strategy, in which the hydroxyl group is converted into a more reactive formylated intermediate prior to $B(C_6F_5)_3$-catalysed reduction (**Fig. 1B**-b).[50] While primary or secondary-selective outcomes are accessible, selective deoxygenation at tertiary alcohol sites or more sterically hindered positions has not been realised within the $B(C_6F_5)_3$/hydrosilane framework (**Fig. 1C**). In addition, existing $B(C_6F_5)_3$-based protocols typically rely on a sacrificial excess of hydrosilane to achieve sufficient reactivity, undermining atom economy and practical utility.[51] Overall, these limitations define a clear selectivity boundary in polyol deoxygenation.

In highly functionalised polyol systems, the intrinsic complexity arising from multiple competing hydroxyl groups can obscure the fundamental origin of site selectivity. To probe this selectivity boundary in a more minimal and well-defined setting, we turned our attention to unsymmetrical diols, which represent the simplest

polyol motifs, while still capturing the key challenges of site discrimination.[52] To overcome the steric constraints inherent to hydride delivery, we devised a carbocation-based pathway that bypasses direct hydride approach and instead leverages electronic stabilization to promote reactivity at hindered sites (**Fig. 1D**). This strategy exploits an S_N1-type mechanism to selectively target sterically encumbered hydroxyl groups, using aryl-substituted diols to stabilize the carbocation intermediate. Complementing this approach, we envisioned the use of a multi-hydride silane as a recyclable hydride donor, enabling a reduction in the excess hydrosilane loading required in earlier $B(C_6F_5)_3$/hydrosilane protocols.

Herein, we disclose a catalytic protocol that enables the regioselective deoxygenation of unsymmetrical diols under remarkably mild conditions (**Fig. 1E**). In contrast to the canonical steric bias of $B(C_6F_5)_3$/hydrosilane systems, selective deoxygenation at sterically encumbered sites is achieved through rational substrate design. The use of substoichiometric hydrosilane represents a notable departure from established $B(C_6F_5)_3$-based protocols and significantly enhances the practicality of the transformation. This feature is particularly advantageous for isotopic labeling, allowing efficient deuterium incorporation with minimal consumption of deuterated silanes. Collectively, these results establish a new reactivity mode within the BCF/silane platform, consistent with carbocation-mediated C–O bond cleavage at electronically stabilised centers.

Results and discussion

Reaction development.

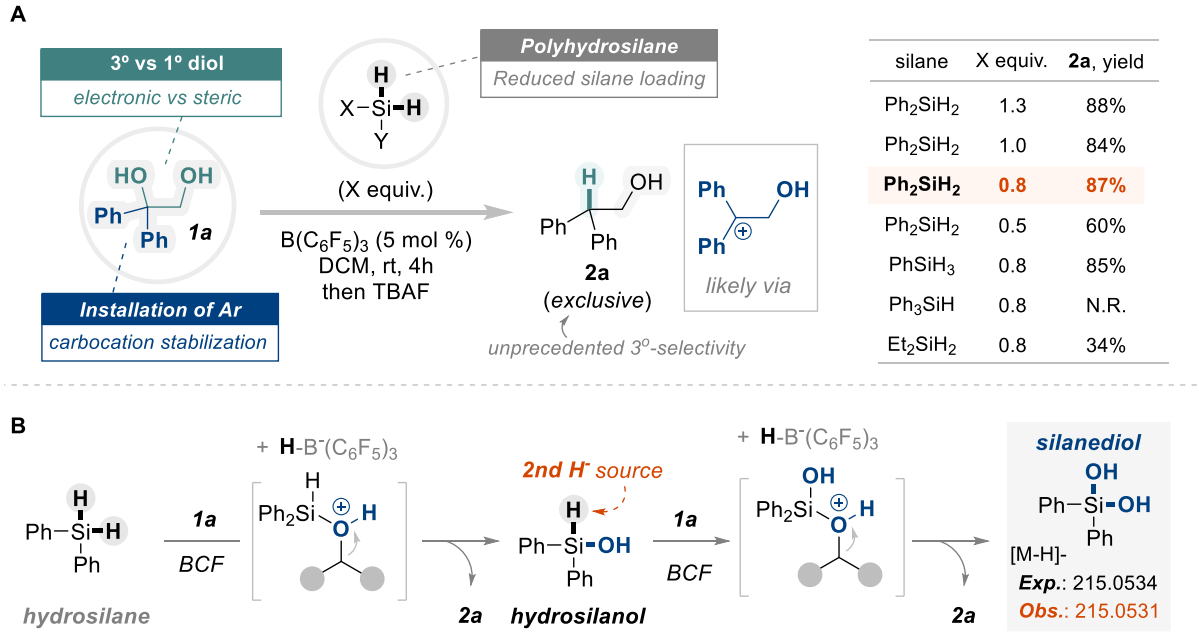


Fig. 2 | Strategic development of regioselective diol deoxygenation via $B(C_6F_5)_3$/hydrosilane catalysis. A. Proof-of-concept reaction design for electronic control of tertiary-selective deoxygenation **B.** Proposed catalytic cycle featuring dual hydride transfer and silane recycling

Guided by this design logic, we examined whether electronic stabilization could override the intrinsic steric bias of $B(C_6F_5)_3$/hydrosilane systems in the deoxygenation of unsymmetrical diols (**Fig. 2A**). To maximize the contrast between the two positions, a 3°/1° diol **1a** was employed as a model substrate, in which the tertiary hydroxyl group bears two aryl substituents to stabilize a developing cationic center, while the primary hydroxyl group remains unsubstituted to minimize competing rearrangement pathways. This design enables a direct comparison between electronic stabilization at the tertiary site and steric accessibility at the primary site.

Delightfully, diol **1a** was converted exclusively to **2a**, the product of the deoxygenation at the sterically hindered tertiary site (see the Supplementary Information for optimised conditions). Such site-selectivity has not been observed in *vicinal* diol systems and suggests that electronic effects may override steric constraints when cationic character is favored.

Alongside the challenge of site-selectivity, the high silane demand characteristic of earlier BCF–hydrosilane protocols posed a significant practical limitation. Within the framework of our designed system, pronounced differences among the hydrosilanes were distinctly revealed. Diphenylsilane stood out by sustaining high reactivity even under substoichiometric conditions, while phenylsilane gave only slightly lower yields and other silanes such as triphenylsilane or diethylsilane exhibited minimal activity. Notably, other Lewis acids tested failed to promote deoxygenation under the same conditions (see the Supplementary Information), underscoring that the $B(C_6F_5)_3$/hydrosilane system operates under unusually mild conditions while requiring only substoichiometric silane loading.

Mechanistic analysis indicated that this unique efficiency arises from the participation of multiple hydride equivalents within the same hydrosilane reagent (**Fig. 2B**). After donating one hydride, diphenylsilane is proposed to generate a hydrosilanol intermediate that can act as an additional hydride donor in a subsequent catalytic cycle. Consistent with this proposal, a silanediol species was detected by high-resolution mass spectrometry (m/z = 215.0531) as a byproduct formed during the reaction. Its presence indicates that a second hydride from the same diphenylsilane molecule had been incorporated, explaining how the system can operate effectively with substoichiometric silane loading.

Substrate scope.

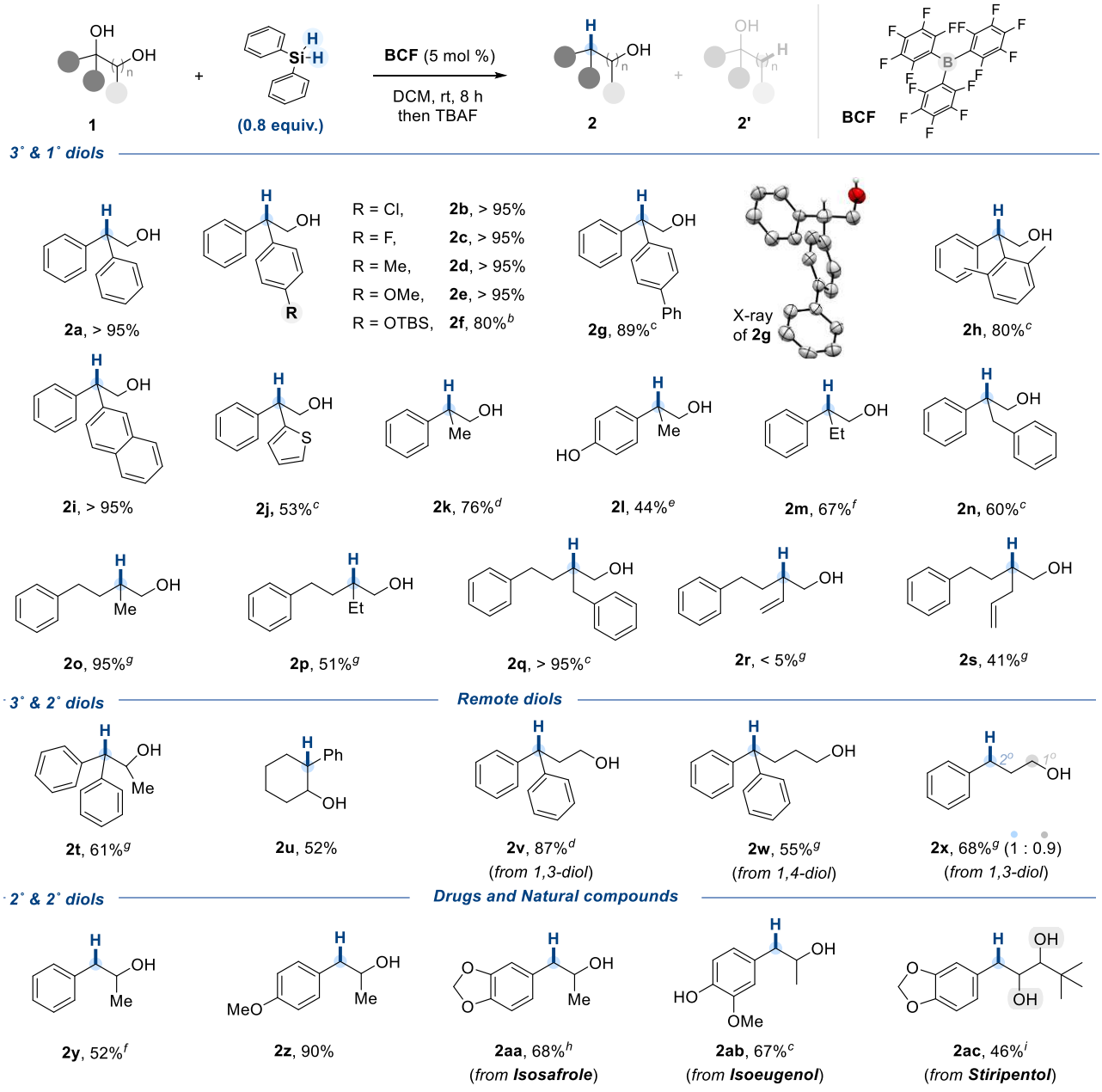
Encouraged by the distinctive site selectivity and silane economy observed in our model studies, we next explored the substrate scope to evaluate the generality and practicality of this method in selective alcohol deoxygenation (**Table 1**). Substrates bearing *para*-substituents underwent smooth deoxygenation to afford the corresponding products in high yields, including electron-withdrawing groups (**2b–2c**) as well as electron-donating groups (**2d–2e**). A silyl ether substituent was also well tolerated (**2f**), demonstrating that the use of hydrosilane as the reductant is compatible with silyl protecting groups. A biphenyl moiety was also tolerated to give high-yielding product **2g**, whose structure was unambiguously confirmed by X-ray crystallographic analysis. Bulky or extended aryl substituents were further accommodated, as exemplified by the *ortho*-dimethyl (**2h**) and naphthyl (**2i**) derivatives, which both gave products in high efficiency. In contrast, the thiophene-containing substrate afforded only a moderate yield (**2j**).

Next, we examined the effect of replacing one of the aryl groups with an aliphatic substituent. Alkyl-substituted substrates bearing methyl, ethyl, or benzyl groups provided the corresponding products (**2k**, **2m**, and **2n**, respectively) with slightly lower efficiency than the diaryl model system. The *para*-hydroxyaryl substrate furnished product **2l**, indicating that a phenolic hydroxyl group is tolerated and that the reaction proceeds in a site- and chemoselective manner, cleaving the tertiary benzylic $C(sp^3)$–OH in the presence of both a primary $C(sp^3)$–OH and an aryl $C(sp^2)$–OH group.

Substrates lacking both aryl substituents furnished products (**2o-2p**) only when phenylsilane ($PhSiH_3$) was used instead of diphenylsilane, whereas the benzyl-containing substrate afforded product **2q** under diphenylsilane conditions. When the vinyl-containing substrate was used, extensive side reactions occurred and the desired product **2r** was not obtained, which may be attributed to a putative carbocation rearrangement arising from the conjugated vinyl group.[53, 54] In contrast, the allyl-containing substrate, which is not susceptible

to such rearrangement, afforded product **2s**, albeit in low yield. Despite these differences in reactivity, the transformation consistently showed high site selectivity for the tertiary benzylic hydroxyl group even in the presence of a sterically accessible primary hydroxyl group.

Table 1. Substrate scope of $B(C_6F_5)_3$/hydrosilane-catalysed site-selective deoxygenation of diols



[a]Reaction conditions: **1** (0.1 mmol), Ph_2SiH_2 (0.8 equiv.), $B(C_6F_5)_3$ (5 mol %) in DCM (0.5 mL) at room temperature for 8 h. Then, TBAF (1.5 equiv.) was added. A single product **2** was furnished unless otherwise indicated. [b]Run for 24 h without TBAF. [c]Run for 24 h. [d]Run at 40 °C. [e]Run with $B(C_6F_5)_3$ (10 mol %), Ph_2SiH_2 (1.0 equiv.) at 40 °C for 24 h. [f]Run with Ph_2SiH_2 (1.3 equiv.) at 40 °C for 24 h. [g]Run with $PhSiH_3$ (1.0 equiv.) for 24 h. [h]$B(C_6F_5)_3$ (10 mol %) for 24 h. [i]Run with Ph_2SiH_2 (1.0 equiv.) for 24 h

To further broaden the scope, we evaluated more structurally diverse types of diols to assess the selectivity and reaction efficiency of this method. Tertiary–secondary diol substrates bearing two aryl /methyl groups or a 1-phenylcyclohexane framework gave products **2t** and **2u**, respectively, both arising from selective deoxygenation at the more substituted tertiary benzylic position, consistent with the general preference for highly substituted centers.

Remote diol substrates bearing 1,3- or 1,4-relationships between hydroxyl groups furnished products **2v** and **2w**, respectively, showing exclusive deoxy-genation at the benzylic site despite the increased distance between hydroxyl groups. Interestingly, when one aryl group was removed from the 1,3-diol scaffold, the corresponding substrate gave product **2x** only under phenylsilane conditions, and the reaction produced a nearly statistical mixture of regioisomers (1:0.9), indicating that the loss of electronic stabilization allowed steric effects to compete and erode site selectivity. We then explored secondary–secondary diols to further assess the scope. A simple 2º/2º diol substrate gave product **2y**, and the *p*-OMe-substituted analogue afforded product **2z** with markedly enhanced reactivity and clear preference for the benzylic site, consistent with electronic stabilization of the developing carbocation by the electron-donating group.

Finally, we demonstrated the applicability of this method to late-stage functionalization of complex natural product or drug derivatives. The isosafrole- and isoeugenol-derived substrates delivered products **2aa** and **2ab**, respectively, both showing selective benzylic deoxygenation, with the latter highlighting that chemoselective transformation of a benzylic hydroxyl group is achievable even in the presence of a phenolic hydroxyl group. It should be highlighted that the stiripentol-derived substrate, bearing three C(sp^3) hydroxyl groups, also underwent highly selective deoxygenation at the benzylic site to form product **2ac**, demonstrating that this method can discriminate among multiple similar hydroxyl groups within a triol framework. Overall, these results demonstrate that this site-selective deoxygenation strategy consistently targets the more substituted benzylic hydroxyl group, even in structurally complex or polyhydroxylated settings, while tolerating diverse electronic and steric environments.

Mechanistic investigation.

The distinct reactivity and site selectivity observed in the substrate scope were reminiscent of the behavior expected from a carbocation intermediate.[55, 56] To verify whether the transformation indeed proceeds through a carbocationic pathway, we conducted mechanistic studies under the standard deoxygenation conditions. Mechanistic insight was first pursued by subjecting substrate **(*R*)-1k**, which contains a chiral center at the tertiary position, to the standard conditions (**Fig. 3A**). The reaction afforded product **2k** in 85% yield as a racemic mixture, and this loss of stereochemical integrity is consistent with an S_N1-type pathway, providing strong evidence for the involvement of a carbocation intermediate.

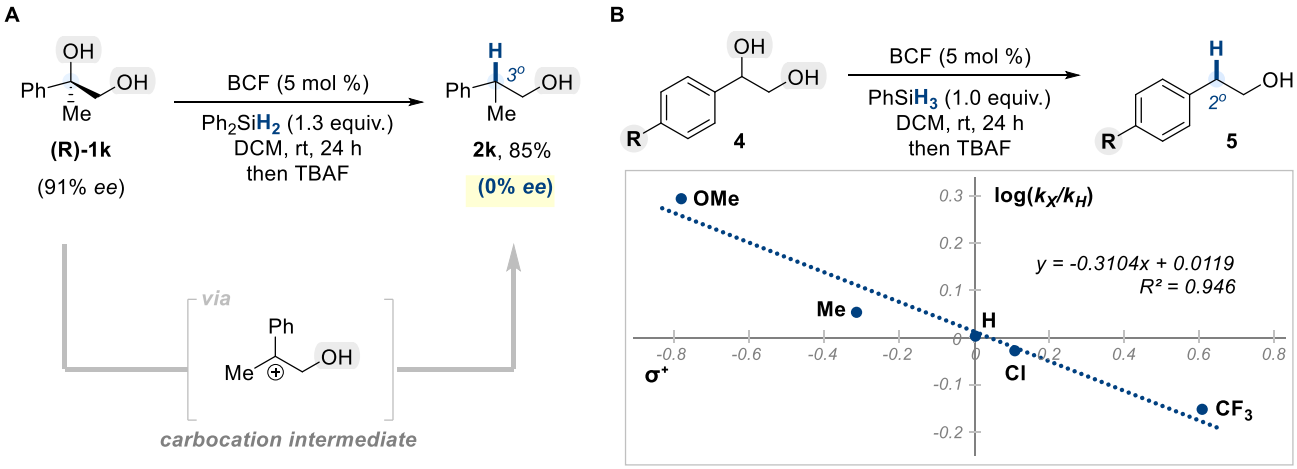


Fig. 3 | **Experimental support for a carbocation pathway. A.** Racemization experiment probing a carbocation-mediated deoxygenation pathway. **B.** Hammett analysis of electronic effects

To further probe the involvement of a carbocation intermediate, we investigated the effect of electronic substituents on the reaction rate through a Hammett analysis (**Fig. 3B**).[57, 58] In contrast to the 3°/1° diols examined in the substrate scope, where the formation of a highly stabilised tertiary carbocation renders the reaction uniformly facile regardless of the substituents, 2°/1° diols provide a more sensitive platform. In these substrates, the benzylic carbocation intermediate is significantly influenced by the electronic nature of the aryl substituent, thereby allowing quantitative evaluation of substituent effects. Diphenylsilane proved unreactive in this system; therefore, stoichiometric phenylsilane (1.0 equiv.) was employed to ensure measurable rates across different substituents. Substrates **4** bearing para-substituents on the aryl ring were subjected to the reaction, and their relative rates were determined. Electron-donating substituents accelerated the transformation, whereas electron-withdrawing groups retarded it, consistent with the accumulation of positive charge in the rate-determining step. A Hammett correlation using σ^+ parameters gave a strong linear relationship with a negative slope ($\rho^+ = -0.31$, $R^2 = 0.946$), indicative of substantial positive charge buildup at the benzylic position. Taken together with the racemization experiment, these results firmly support that the transformation proceeds through a carbocationic pathway, with both stereochemical scrambling and substituent-dependent reactivity providing convergent mechanistic evidence.

Having established that the reaction proceeds through a carbocation intermediate, we next examined how such a species could be generated under our catalytic conditions (**Fig. 4A**). In the system reported by Morandi and co-workers,[43, 44] the hydrosilane engages both hydroxyl groups of a 1,2-diol to form a cyclic siloxane intermediate, thereby consuming all available hydride equivalents and necessitating an additional equivalent of hydrosilane to complete deoxygenation. By contrast, in our system, substoichiometric diphenylsilane alone is sufficient to achieve both deoxygenation and hydride delivery. This fundamental difference strongly suggests that a cyclic siloxane intermediate is unlikely to be operative under our conditions, rendering the cyclic pathway implausible. To rationalize the observed outcome, we instead considered two acyclic scenarios. In the first, initial silylation occurs at the primary hydroxyl group, giving a silyl oxonium intermediate. Our racemization study revealed that the tertiary benzylic position undergoes racemization, which clearly points to the formation of a benzylic carbocation in this system. Therefore, if silylation were to occur at the primary site, a rearrangement step would be required to generate the benzylic carbocation. In the second scenario, silylation takes place directly at the tertiary hydroxyl group, triggering spontaneous departure of the leaving group and direct carbocation formation, which then undergoes deoxygenation to furnish product **2a**.

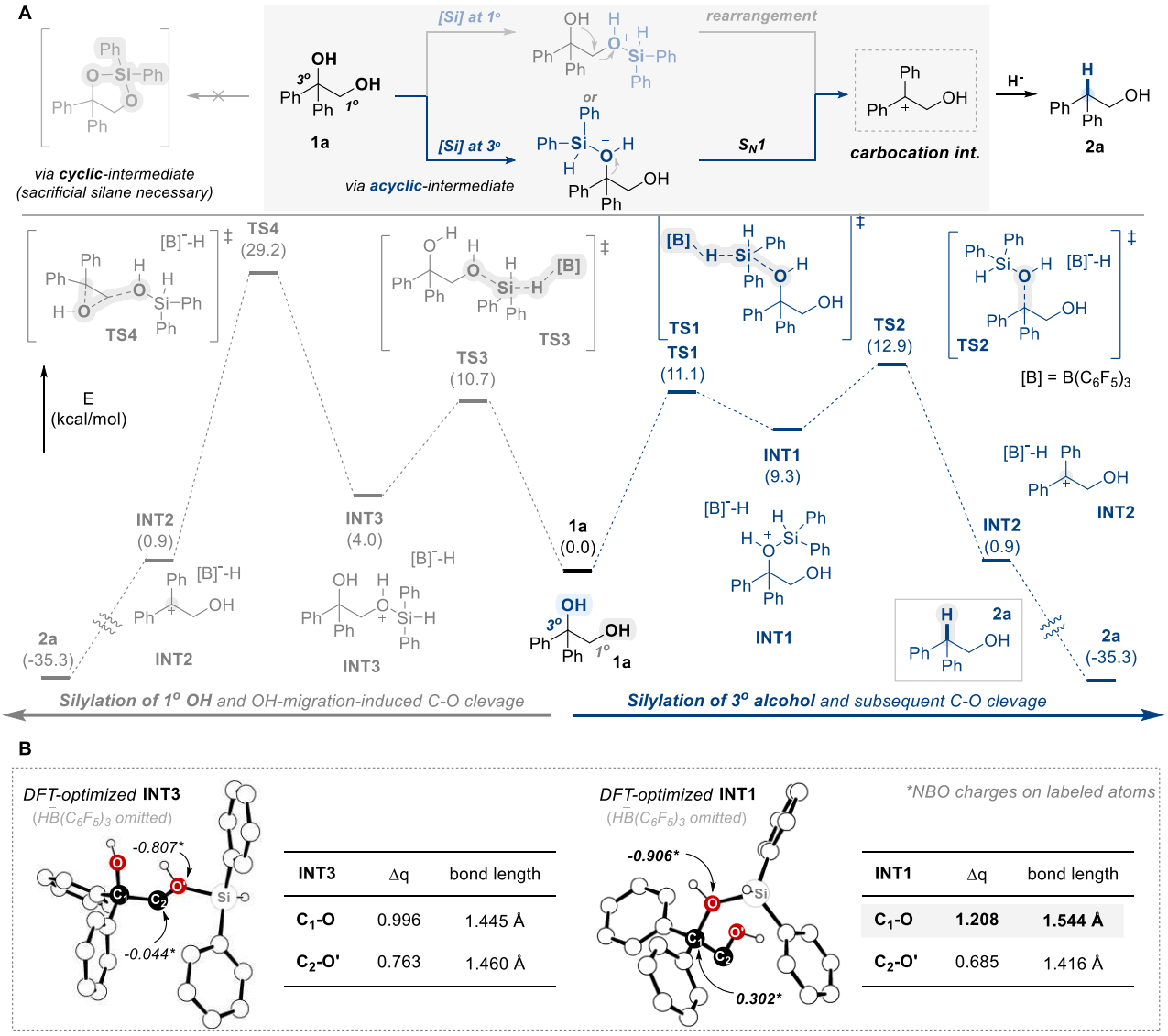


Fig. 4 | DFT analysis of site-selective silylation in 3°/1° diol. **A.** Comparison of competing silylation pathways leading to C–O bond cleavage **B.** DFT analysis of electronic differentiation between key intermediates

DFT calculations were performed to compare these two pathways. In the first step, the barrier for Si–O bond formation at the primary hydroxyl group (**TS3**, 10.7 kcal/mol) is slightly lower than that at the tertiary hydroxyl group (**TS1**, 11.1 kcal/mol), consistent with the greater steric accessibility of the primary position. The resulting intermediates also exhibit a thermodynamic preference for the primary silylated species (**INT3**, 4.0 kcal/mol) over the tertiary counterpart (**INT1**, 9.3 kcal/mol), reflecting steric congestion around the tertiary silyloxonium center. The decisive distinction between the two pathways, however, emerges in the subsequent step: departure of the leaving group via **TS2** in the tertiary pathway requires only 12.9 kcal/mol, whereas rearrangement through **TS4** in the primary pathway demands 29.2 kcal/mol. Taken together, this analysis indicates that, although primary silylation is both kinetically and thermodynamically accessible, equilibration between the two silylated intermediates would ultimately funnel the reaction toward tertiary silylation, from which the S_N1-type deoxygenation proceeds through the energetically more favorable **TS1–TS2** sequence.

To complement these energetic comparisons, we next examined the electronic and structural features of the silyloxonium intermediates (**Fig. 4B**), focusing on the natural bond orbital (NBO) charge distribution and

bond metrics at the ionizing C–O bond. The tertiary silyloxonium **INT1** (Δq = 1.208) exhibits markedly greater polarization across the C–O bond than the primary-silylated **INT3** (Δq = 0.996), indicating stronger predisposition toward heterolysis. Consistently, the cleaving C–O bond in **INT1** (1.544 Å) is elongated relative to **INT3** (1.445 Å), further reflecting its weakened character. These combined electronic and structural features explain why tertiary silyloxonium **INT1** is primed to undergo direct carbocation formation through **TS2**, whereas **INT3**, with its less polarised and shorter C–O bond, requires a high-energy rearrangement via **TS4**.

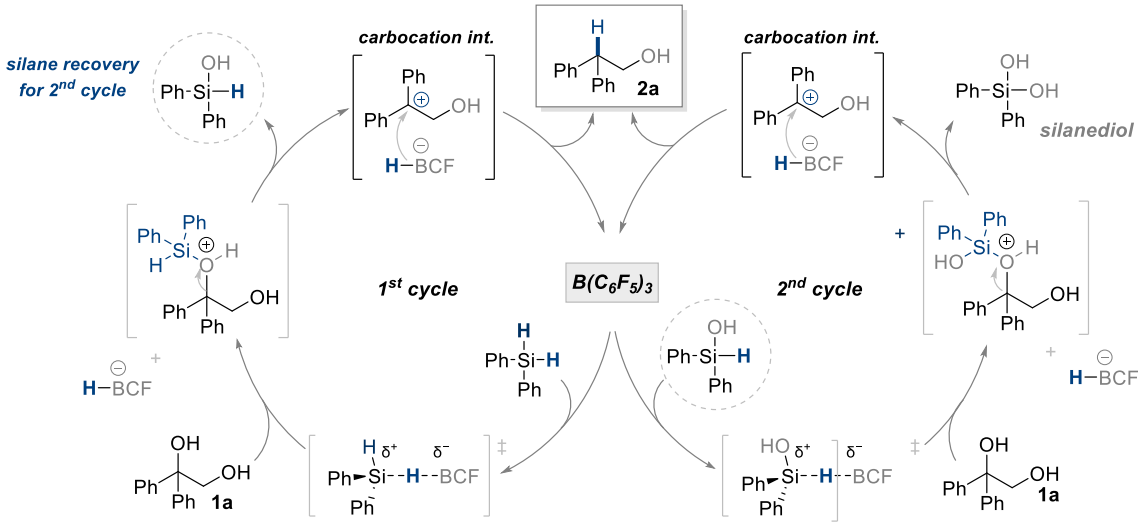
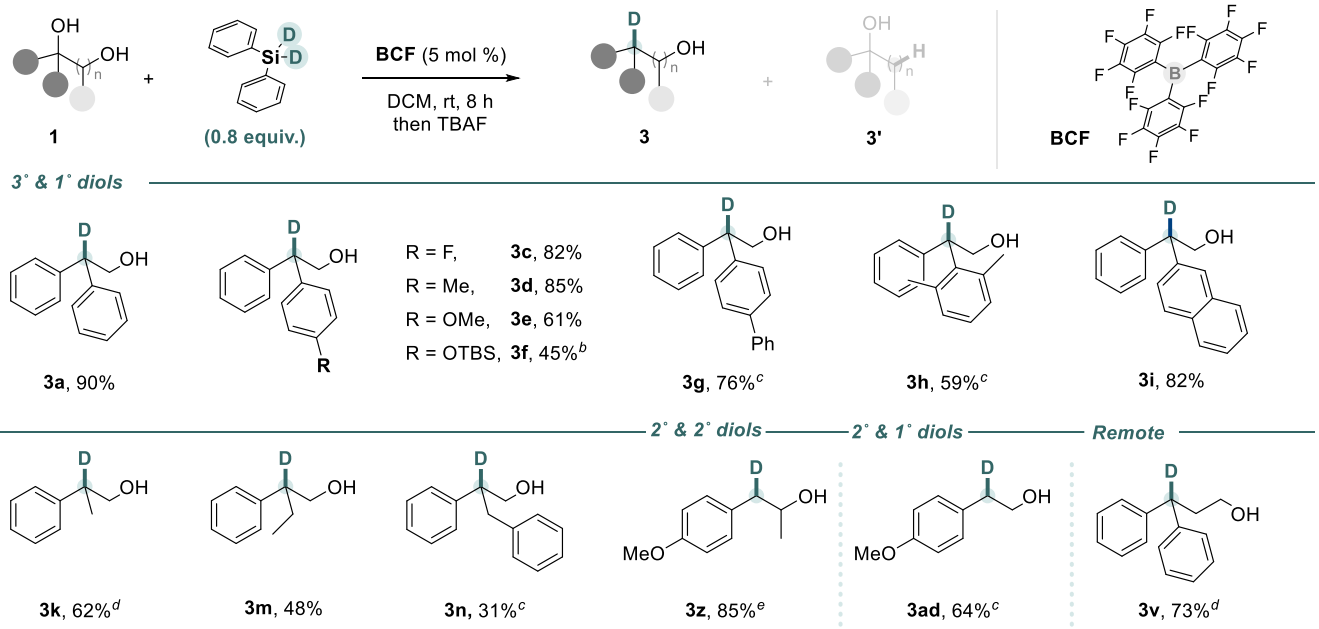


Fig. 5 | Plausible Reaction Mechanism

On the basis of experimental and computational studies, a plausible reaction mechanism was proposed (**Fig. 5**). The process is delineated as proceeding through two sequential cycles that collectively rationalize the substoichiometric use of diphenylsilane. In the first cycle, interaction between $B(C_6F_5)_3$ and diphenylsilane activates the hydrosilane through polarization of the Si–H bond, thereby enabling silylation of the diol substrate. This silylation is proposed to occur preferentially at the tertiary hydroxyl group, as supported by DFT analysis. The resulting silyl oxonium species undergoes C–O bond cleavage to generate a benzylic carbocation, whose formation was further corroborated by the racemization and Hammett analysis. This carbocation intermediate is subsequently quenched by delivery of a polarised hydride from the $B(C_6F_5)_3$-activated diphenylsilane, affording the deoxygenated product **2a** along with a silanol species.

In the second cycle, an analogous process is proposed to occur in which the silanol functions as an additional hydride source. Through the same sequence of $B(C_6F_5)_3$-mediated activation and hydride transfer, silanediol is produced as the terminal byproduct derived from hydrosilane. The formation of silanediol was independently confirmed by HRMS analysis, thereby providing experimental support for the proposed two-step silane oxidation sequence and accounting for the high silane economy observed under the reaction conditions. Given that our protocol operates with substoichiometric amounts of hydrosilane while maintaining high site selectivity, we envisioned that the same manifold could be exploited for isotopic labeling. Benzylic deuterium incorporation is particularly valuable for mechanistic investigations and tracer studies,[59] yet existing methods often require harsh conditions or an excess of deuterium sources.[60] Our catalytic system offered the opportunity to achieve this transformation under mild and efficient conditions.

Table 2. $B(C_6F_5)_3$-catalysed site-selective benzylic deuteration



[a]Reaction conditions: **1** (0.1 mmol), Ph_2SiD_2 (0.8 equiv.), $B(C_6F_5)_3$ (5 mol %) in DCM (0.5 mL) at room temperature for 8 h. Then, TBAF (1.5 equiv.) was added. A single product **3** was furnished unless otherwise indicated. [b]Run for 24 h without TBAF. [c]Run for 24 h. [d]Run at 40 °C.

Accordingly, diphenylsilane-d_2 was employed as the reductant, and a range of diol substrates were examined (**Table 2**). Delightfully, the model tertiary-primary diol **1a** underwent smooth deuteration to give **3a** in 90% yield. *Para*-substituted aryl diols furnished the corresponding products **3c**-**3e** in moderate to high yields, regardless of whether electron-withdrawing or electron-donating groups were present. Substrates bearing additional functional motifs, including an OTBS-protected alcohol, a biphenyl unit, and a naphthyl group, also underwent efficient transformation to deliver products (**3f-3i**). In contrast, substrates bearing simple alkyl substituents at the tertiary center gave **3k-3n** in diminished efficiencies. Further extension to other diol classes provided **3z**, **3ad**, and **3v** from secondary-secondary, secondary-primary, and remote diols, respectively.

Although the yields were somewhat lower than those achieved in the hydride delivery manifold, the transformation consistently provided high site selectivity for benzylic deuteration. This protocol therefore establishes a mild, practical, and reagent-efficient entry to benzylic deuterium-labeled molecules, offering a powerful tool for mechanistic studies and isotopic tracer applications.

Conclusions

In summary, we have developed a $B(C_6F_5)_3$/hydrosilane catalytic system that enables regioselective deoxygenation of unsymmetrical diols under mild conditions. Unlike conventional methods that preferentially target sterically accessible sites, this strategy exploits carbocation intermediacy to achieve C–O bond cleavage at sterically demanding positions. Mechanistic studies combining experiment and computation established that the reaction proceeds via acyclic silyloxonium intermediates and carbocation formation, with polarization and bond weakening at tertiary sites accounting for the observed selectivity.

Diphenylsilane was identified as the optimal reductant, functioning both as an activator and a dual hydride donor, ensuring high silane economy. The method exhibits broad substrate scope, encompassing diverse classes of diols as well as natural product derivatives. Furthermore, its extension to site-selective benzylic deuteration provides a mild entry to isotopically labeled molecules, underscoring the versatility of this

platform. Collectively, these findings establish a practical framework for site-selective alcohol deoxygenation and open new opportunities for advancing selective C–O bond cleavage chemistry

Methods

General procedure. In an argon-filled glovebox, diols (0.10 mmol, 1.0 equiv.) and $B(C_6F_5)_3$ (5 mol%) were dissolved in dichloromethane (0.5 mL) in a 4 mL screw-cap vial equipped with a magnetic stir bar. The hydrosilane was added dropwise, and the reaction mixture was stirred at room temperature for 8 h. The reaction was quenched with a TBAF solution (1.5 equiv.), and the crude mixture was purified by the flash column chromatography on silica gel using hexane/ethyl acetate (95:5, v/v) as the eluent to afford the desired products.

Data Availability. Materials and methods, experimental procedures, mechanistic studies, characterization data, spectral data, and Cartesian coordinates associated with computational studies are available in the Supplementary Information. Crystallographic data for compound **2g** have been deposited with the Cambridge Crystallographic Data Centre under deposition number CCDC 2501997.

References

1. Shugrue, C. R., Miller, S. J. Applications of nonenzymatic catalysts to the alteration of natural products. *Chem. Rev.* **117**, 11894-11951 (2017).
2. Dethlefsen, J. R., Lupp, D., Teshome, A., Nielsen, L. B., Fristrup, P. Molybdenum-catalyzed conversion of diols and biomass-derived polyols to alkenes using isopropyl alcohol as reductant and solvent. *ACS Catal.* **5**, 3638-3647 (2015).
3. Seo, Y., Lowe, J. M., Gagné, M. R. Controlling sugar deoxygenation products from biomass by choice of fluoroarylborane catalyst. *ACS Catal.* **9**, 6648-6652 (2019).
4. McDonald, T. R., Mills, L. R., West, M. S., Rousseaux, S. A. L. Selective carbon–carbon bond cleavage of cyclopropanols. *Chem. Rev.* **121**, 3-79 (2021).
5. Beale, T. M., Taylor, M. S. Synthesis of cardiac glycoside analogs by catalyst-controlled, regioselective glycosylation of digitoxin. *Org. Lett.* **15**, 1358-1361 (2013).
6. Hill, C. K., Hartwig, J. F. Site-selective oxidation, amination and epimerization reactions of complex polyols enabled by transfer hydrogenation. *Nat. Chem.* **9**, 1213-1221 (2017).
7. Fowler, B. S., Laemmerhold, K. M., Miller, S. J. Catalytic site-selective thiocarbonylations and deoxygenations of vancomycin reveal hydroxyl-dependent conformational effects. *J. Am. Chem. Soc.* **134**, 9755-9761 (2012).
8. Loh, C. C. J. Synergistic catalysis: An emerging concept for selective carbohydrate synthesis. *Chem Catal.* **4**, (2024).
9. Snyder, S. A., Gollner, A., Chiriac, M. I. Regioselective reactions for programmable resveratrol oligomer synthesis. *Nature* **474**, 461-466 (2011).
10. Cook, A., Newman, S. G. Alcohols as substrates in transition-metal-catalyzed arylation, alkylation, and related reactions. *Chem. Rev.* **124**, 6078-6144 (2024).
11. Jiang, Y. et al. Direct radical functionalization of native sugars. *Nature* **631**, 319-327 (2024).
12. Kulkarni, S. S., Wang, C.-C., Sabbavarapu, N. M., Podilapu, A. R., Liao, P.-H., Hung, S.-C. "One-pot" protection, glycosylation, and protection–glycosylation strategies of carbohydrates. *Chem. Rev.* **118**, 8025-8104 (2018).
13. Tang, H., Tian, Y.-B., Cui, H., Li, R.-Z., Zhang, X., Niu, D. Site-switchable mono-o-allylation of polyols. *Nat. Commun.* **11**, 5681 (2020).

14. Rao, V. U. B. et al. A synergistic Rh(i)/organoboron-catalysed site-selective carbohydrate functionalization that involves multiple stereocontrol. *Nat. Chem.* **15**, 424-435 (2023).

15. Yamatsugu, K., Kanai, M. Catalytic approaches to chemo- and site-selective transformation of carbohydrates. *Chem. Rev.* **123**, 6793-6838 (2023).

16. Dimakos, V., Taylor, M. S. Site-selective functionalization of hydroxyl groups in carbohydrate derivatives. *Chem. Rev.* **118**, 11457-11517 (2018).

17. Chung, K. et al. Chemoselective Pd-catalyzed oxidation of polyols: Synthetic scope and mechanistic studies. *J. Am. Chem. Soc.* **135**, 7593-7602 (2013).

18. Guo, H., Kirchhoff, J.-L., Strohmann, C., Grabe, B., Loh, C. C. J. Asymmetric Pd/organoboron-catalyzed site-selective carbohydrate functionalization with alkoxyallenes involving noncovalent stereocontrol. *Angew. Chem. Int. Ed.* **63**, e202400912 (2024).

19. Loh, C. C. J. Catalytic strategies for stereoselective carbohydrate synthesis: Emerging concepts for accessing challenging glycosides. *Angew. Chem. Int. Ed.* **64**, e202514167 (2025).

20. Sebastian, A. T., Loh, C. C. J. Emerging capabilities of nonclassical noncovalent interactions and asymmetric catalysis in stereoselective glycosylations and carbohydrate functionalizations. *Acc. Chem. Res.* **58**, 2124-2144 (2025).

21. Clarke, J. J., Basemann, K., Romano, N., Lee, S. J., Gagné, M. R. Borane- and silylium-catalyzed difunctionalization of carbohydrates: 3,6-anhydrosugar enabled 1,6-site selectivity. *Org. Lett.* **24**, 4135-4139 (2022).

22. Wan, W., Ammal, S. C., Lin, Z., You, K.-E., Heyden, A., Chen, J. G. Controlling reaction pathways of selective C–O bond cleavage of glycerol. *Nat. Commun.* **9**, 4612 (2018).

23. Guo, H.-M., Wu, X. Selective deoxygenative alkylation of alcohols via photocatalytic domino radical fragmentations. *Nat. Commun.* **12**, 5365 (2021).

24. Dai, X.-J., Li, C.-J. En route to a practical primary alcohol deoxygenation. *J. Am. Chem. Soc.* **138**, 5433-5440 (2016).

25. Williams, O. P., Chmiel, A. F., Mikhael, M., Bates, D. M., Yeung, C. S., Wickens, Z. K. Practical and general alcohol deoxygenation protocol. *Angew. Chem. Int. Ed.* **62**, e202300178 (2023).

26. Bender, T. A., Dabrowski, J. A., Gagné, M. R. Homogeneous catalysis for the production of low-volume, high-value chemicals from biomass. *Nat. Rev. Chem.* **2**, 35-46 (2018).

27. Fang, H., Oestreich, M. Defunctionalisation catalysed by boron lewis acids. *Chem. Sci.* **11**, 12604-12615 (2020).

28. Herrmann, J. M., König, B. Reductive deoxygenation of alcohols: Catalytic methods beyond barton–mccombie deoxygenation. *Eur. J. Org. Chem.* **2013**, 7017-7027 (2013).

29. Yasuda, M., Onishi, Y., Ueba, M., Miyai, T., Baba, A. Direct reduction of alcohols: highly chemoselective reducing system for secondary or tertiary alcohols using chlorodiphenylsilane with a catalytic amount of indium trichloride. *J. Org. Chem.* **66**, 7741-7744 (2001).

30. Miyai, T., Ueba, M., Baba, A. Novel synthetic usage of indium compounds as catalyst: Reductive deoxygenation of aryl ketones and sec-benzylic alcohols. *Synlett* **1999**, 182-184 (1999).

31. Sakai, N., Nagasawa, K., Ikeda, R., Nakaike, Y., Konakahara, T. $InBr_3$-catalyzed reduction of ketones with a hydrosilane: Deoxygenation of aromatic ketones and selective synthesis of secondary alcohols and symmetrical ethers from aliphatic ketones. *Tetrahedron Lett.* **52**, 3133-3136 (2011).

32. Baba, A., Yasuda, M., Nishimoto, Y., Saito, T., Onishi, Y. Reaction of alcohols and silyl ethers in the presence of an indium/silicon-based catalyst system: Deoxygenation and allyl substitution. *Pure Appl. Chem.* **80**, 845-854 (2008).

33. Sawadjoon, S., Lundstedt, A., Samec, J. S. M. Pd-catalyzed transfer hydrogenolysis of primary, secondary, and tertiary benzylic alcohols by formic acid: A mechanistic study. *ACS Catal.* **3**, 635-642 (2013).

34. Buhaibeh, R., Thyagarajan, N., Bousrez, G., Monsigny, L., Cantat, T., Nicolas, E. Scandium-catalyzed highly selective deoxygenation of alcohols by using hydrosilanes as reductants. *Chem. Eur. J.* **31**, e202501596 (2025).

35. Lin, Q., Tong, W., Shu, X.-Z., Chen, Y. Ti-catalyzed dehydroxylation of tertiary alcohols. *Org. Lett.* **24**, 8459-8464 (2022).

36. Căciuleanu, A., Vöhringer, F., Fleischer, I. Titanium-catalysed deoxygenation of benzylic alcohols and lignin model compounds. *Org. Chem. Front.* **10**, 2927-2935 (2023).

37. Adduci, L. L., McLaughlin, M. P., Bender, T. A., Becker, J. J., Gagné, M. R. Metal-free deoxygenation of carbohydrates. *Angew. Chem. Int. Ed.* **53**, 1646-1649 (2014).

38. Drosos, N., Cheng, G.-J., Ozkal, E., Cacherat, B., Thiel, W., Morandi, B. Catalytic reductive pinacol-type rearrangement of unactivated 1,2-diols through a concerted, stereoinvertive mechanism. *Angew. Chem. Int. Ed.* **56**, 13377-13381 (2017).

39. Yang, W., Gao, L., Lu, J., Song, Z. Chemoselective deoxygenation of ether-substituted alcohols and carbonyl compounds by $B(C_6F_5)_3$-catalyzed reduction with $(HMe_2SiCH_2)_2$. *Chem. Commun.* **54**, 4834-4837 (2018).

40. Drosos, N., Ozkal, E., Morandi, B. Catalytic selective deoxygenation of polyols using the B $(C_6F_5)_3$/silane system. *Synlett* **27**, 1760-1764 (2016).

41. Gevorgyan, V., Rubin, M., Benson, S., Liu, J.-X., Yamamoto, Y. A novel $B(C_6F_5)_3$-catalyzed reduction of alcohols and cleavage of aryl and alkyl ethers with hydrosilanes. *J. Org. Chem.* **65**, 6179-6186 (2000).

42. Gevorgyan, V., Liu, J.-X., Rubin, M., Benson, S., Yamamoto, Y. A novel reduction of alcohols and ethers with a HSiEt catalytic $B(C_6F_5)_3$ system. *Tetrahedron Lett.* **40**, 8919-8922 (1999).

43. Drosos, N., Morandi, B. Boron-catalyzed regioselective deoxygenation of terminal 1,2-diols to 2-alkanols enabled by the strategic formation of a cyclic siloxane intermediate. *Angew. Chem. Int. Ed.* **54**, 8814-8818 (2015).

44. Cheng, G.-J., Drosos, N., Morandi, B., Thiel, W. Computational study of $B(C_6F_5)_3$-catalyzed selective deoxygenation of 1, 2-diols: Cyclic and noncyclic pathways. *ACS Catal.* **8**, 1697-1702 (2018).

45. Chatterjee, I., Porwal, D., Oestreich, M. $B(C_6F_5)_3$-catalyzed chemoselective defunctionalization of ether-containing primary alkyl tosylates with hydrosilanes. *Angew. Chem. Int. Ed.* **56**, 3389-3391 (2017).

46. Seo, Y., Gagné, M. R. Positional selectivity in the hydrosilylative partial deoxygenation of disaccharides by boron catalysts. *ACS Catal.* **8**, 81-85 (2018).

47. Bender, T. A., Dabrowski, J. A., Gagné, M. R. Delineating the multiple roles of $B(C_6F_5)_3$ in the chemoselective deoxygenation of unsaturated polyols. *ACS Catal.* **6**, 8399-8403 (2016).

48. Oestreich, M., Hermeke, J., Mohr, J. A unified survey of Si–H and H–H bond activation catalysed by electron-deficient boranes. *Chem. Soc. Rev.* **44**, 2202-2220 (2015).

49. Seo, Y., Gudz, A., Lowe, J. M., Gagné, M. R. Selective deoxygenation of gibberellic acid with fluoroarylborane catalysts. *Synthesis* **75**, 130712 (2019).

50. Richter, S. C., Oestreich, M. Chemoselective deoxygenation of 2° benzylic alcohols through a sequence of formylation and $B(C_6F_5)_3$-catalyzed reduction. *Eur. J. Org. Chem.* **2021**, 2103-2106 (2021).

51. Hackel, T., McGrath, N. A. Tris(pentafluorophenyl)borane-catalyzed reactions using silanes. *Molecules* **24**, 432 (2019).

52. Niaz, L., Bang, S., Lee, J. Recent progress in selective functionalization of diols via organocatalysis. *Org. Chem. Front.* **12**, 5072-5104 (2025).

53. Fu, L., Damsen, H., Niggemann, M. A vinyl-cation-induced 1,3-aryl shift. *Chem. Eur. J.* **23**, 12158-12161 (2017).

54. Cleary, S. E., Hensinger, M. J., Qin, Z.-X., Hong, X., Brewer, M. Migratory aptitudes in rearrangements of destabilized vinyl cations. *J. Org. Chem.* **84**, 15154-15164 (2019).

55. Naredla, R. R., Klumpp, D. A. Contemporary carbocation chemistry: Applications in organic synthesis. *Chem. Rev.* **113**, 6905-6948 (2013).

56. Adams, H. K., Kadarauch, M., Hodson, N. J., Lit, A. R., Phipps, R. J. Design approaches that utilize ionic interactions to control selectivity in transition metal catalysis. *Chem. Rev.* **125**, 2846-2907 (2025).

57. Kumar, G. et al. Evaluating differences in the active-site electronics of supported au nanoparticle catalysts using hammett and dft studies. *Nat. Chem.* **10**, 268-274 (2018).

58. Nguyen, N.-H., Apriletti, J. W., Baxter, J. D., Scanlan, T. S. Hammett analysis of selective thyroid hormone receptor modulators reveals structural and electronic requirements for hormone antagonists. *J. Am. Chem. Soc.* **127**, 4599-4608 (2005).

59. Kopf, S., Bourriquen, F., Li, W., Neumann, H., Junge, K., Beller, M. Recent developments for the deuterium and tritium labeling of organic molecules. *Chem. Rev.* **122**, 6634-6718 (2022).

60. Atzrodt, J., Derdau, V., Kerr, W. J., Reid, M. Deuterium- and tritium-labelled compounds: Applications in the life sciences. *Angew. Chem. Int. Ed.* **57**, 1758-1784 (2018).

Acknowledgements

This work was supported by the National Research Foundation of Korea (NRF) grant funded by the Korea government (MSIT). (RS-2024-00342503). The authors gratefully acknowledge Dr. Dongwook Kim (IBS) for single-crystal X-ray diffraction experiments. Computational studies for this research were performed on the High Performance Computing Resources in the IBS Research Solution Center.

Author contributions

Experiment, S.B., J.L., D.J., and Y.K.; Computation, J.L.*; Manuscript, S.B. and J.L.*

Competing interests

The authors declare no competing interests.

Additional information

Supplementary information is available in the online version of the paper. Reprints and permissions information is available at www.nature.com/reprints. Correspondence and requests for the materials should be addressed to J.L.*

Supplementary Files

This is a list of supplementary files associated with this preprint. Click to download.

- SIsubmitted.pdf